ELSEVIER

Polymer 40 (1999) 1201–1208

polymer

Effect of casting solvents on physical properties of hydrogenated styrene–butadiene copolymer

Mousumi De Sarkar, Prajna P. De, Anil K. Bhowmick*

Rubber Technology Centre, Indian Institute of Technology, Kharagpur, West Bengal 721302, India

Received 16 December 1997; revised 13 March 1998; accepted 22 April 1998

Abstract

The effect of casting solvents on swelling resistance, crystallinity, dynamic mechanical, and mechanical properties of hydrogenated styrene butadiene copolymer (HSBR) has been investigated. The solvents chosen are cyclohexane, carbon tetrachloride, toluene and chloroform, which cover a range of solubility parameters from 8.2 to 9.3 $(cal/cm^3)^{1/2}$. The crystallinity, swelling resistance and mechanical properties are maximum with cyclohexane cast films. The dynamic mechanical properties, tan δ and E', are also influenced by the nature of the solvents. Cyclohexane cast films have the highest values of dynamic modulus. For comparison, compression moulded film has also been studied. The properties of the samples have been correlated with the structure. The properties of the films are also dependent on solvent evaporation rate.

Keywords: Hydrogenated styrene–butadiene copolymer; Solvent casting; Dynamic mechanical properties

1. Introduction

Of late, chemical modification of diene elastomers has emerged as an active field of research because of the technological importance of the modified products. Hydrogenation is one of the most important methods for improving and changing the properties of an existing unsaturated elastomer [1]. Hydrogenated styrene–butadiene rubber (HSBR) via diimide reduction technique has been reported recently [2]. SBR latex is not only efficiently hydrogenated by this technique, but is also found to be a unique thermoplastic elastomer due to its crystalline polyethylene segments [3]. We have reported earlier on preparation, characterisation and several properties of HSBR [4,5]. However, to the best of our knowledge, no work has been done on the solution properties of HSBR. Also, there is no study reported in the literature on the influence of casting solvents on the properties of HSBR. It is widely recognized that solvent quality determines the chain configuration of macromolecules in solution [6]. Consequently, it might be expected that this polymer–solvent interaction would also affect the manner in which polymer chains pack together in the film and therefore, influence its properties. It is also worth mentioning that the mechanical properties of HSBR need further improvement and one of the ways may be to increase crystalline packing of polymer chains.

In this article, we report on the physical properties of HSBR films cast from various solutions. The polymer has different configurations in these solvents as judged from the intrinsic viscosity data. The solvents investigated, covering a range [8.2–9.3 $(cal/cm^3)^{1/2}$] of solubility parameters, were cyclohexane, carbon tetrachloride, toluene and chloroform. All these solvents fall in the poor hydrogen bonding class. The copolymer was, of course, soluble to different extents in each of the solvents. For comparison purposes, a compression moulded film of HSBR was used as the control.

2. Experimental

2.1. Materials

Hydrogenated styrene–butadiene elastomer (94% saturated) was prepared by diimide reduction of SBR latex with 17% styrene content, obtained from Nippon Zeon, Japan. The details of the hydrogenation process were described elsewhere [4]. Polymer characterisation data are shown in Table 1. Solvents used (cyclohexane, carbon tetrachloride, toluene and chloroform) were of spectroquality grade. Table 2 details the characteristics of the solvents.

* Corresponding author.

0032-3861/98/$ - see front matter
PII S0032-3861(98)00338-3

Table 1
Polymer characterisation data

	HSBR-94[a]
Wt. % of styrene[b]	17.1
$M_n \times 10^{-4}$	2.33
$M_w \times 10^{-4}$	6.20
M_w/M_n	2.66
Configuration analysis[b]	
% *cis*	9.5
% *trans*	56.7
% vinyl	16.7
Density (g/cm^3)	0.933

[a] HSBR with 94% saturation
[b] Calculated from IR spectra

2.2. Preparation of films

Approximately 4% w/v solutions in redistilled solvents (cyclohexane, CCl_4, toluene and chloroform) were cast into clean plate-glass trays where the rate of evaporation could be controlled by varying the rate of flow of air over the surface of evaporating liquid at 25°C. Considerable care was taken to remove the last trace of solvents before any physical measurements were undertaken. This was checked gravimetrically by taking the weight of the films to constant weight. The properties of the films measured at wide intervals of time (3 months) were the same and reproducible. Since the films were prepared by solvent evaporation and not annealed, they may have been in non-equilibrium states. This was not considered important for the present investigation, as the focus was to study the effect of casting solvents. The data, however, are reproducible and valid.

Compression moulded films of about 0.2 mm thickness were formed at 150°C at a pressure of 5 tons in an electrically heated Moore press between two aluminium foils.

2.3. Measurement of viscosity

Viscosity measurements were carried out at a temperature of 27 ± 1°C in an Ostwald viscometer. The average flow times of these measurements were taken. Data on different concentrations were plotted using the relations [7,8] as shown in Eqs. (1) and (2):

$$\eta_{sp}/C = [\eta] + K_H[\eta]^2 C \quad (1)$$

$$\ln \eta_r/C = [\eta] - \left(\frac{1}{2} - K_H\right)[\eta]^2 C \quad (2)$$

where η_{sp} and η_r are the specific viscosity and relative viscosity respectively and C is the concentration. General extrapolations based on the above two equations give the value of intrinsic viscosity $[\eta]$ and the Huggins constant, K_H from the intercepts and slopes respectively. The dimension of the chains was measured from the viscosity data by using Flory's equation [6]

$$[\eta] = \phi(\bar{h}^2)^{3/2}/M \quad (3)$$

where M is the molecular weight, ϕ is a constant (equal to 2.1×10^{21} with $[\eta]$ in 100 ml g^{-1} for a number of linear macromolecules) and $(\bar{h}^2)^{1/2}$ is the root mean square end-to-end distance (cm).

2.4. Transmission electron microscopic (TEM) and scanning electron microscopic (SEM) studies

The microstructure of the cast and moulded films was analysed using a Transmission Electron Microscope (TEM, Philips, CM-12 model, 40 kV, operating voltage) and a Scanning Electron Microscope (SEM, Hitachi, S415A model). For TEM observation, a 0.08% w/v solution was first made. The films were cast directly onto the copper grid as well as into water [9]. The rubber was then stained with osmium tetroxide for better contrast. The osmium tetraoxide stained samples were also examined under SEM after coating the sample with gold in a sputter machine. Secondary electron images were taken.

2.5. Wide angle x-ray diffraction studies (WAXS)

The films were subjected to Iron filtered Co-K_α radiation generated from a Philips PW 1719 x-ray generator at an operating voltage and current of 40 kV and 20 mA respectively. The diffraction pattern of the samples was recorded with a Philips x-ray diffractometer (PW 1710). Films of the same thickness and the same area were exposed. The diffractions were recorded in an angular range from 10° 2θ to 50° 2θ at a scanning speed of 3°/min. The amorphous reflection contributions were subsequently resolved with curve fitting by a non-linear least square method under the assumption that the intensity peak profile could be approximated by a Gaussian function [10]. The degree of crystallinity was determined from the ratio of areas under the crystalline peaks and the amorphous halo. For the purpose of indexing the reflections, the interplanar distance, d_{hkl}, was

Table 2
Characteristics of casting solvents

Solvent	Solubility parameter (cal/cm^3)$^{1/2}$	Boiling point (°C)	Heat of vaporisation at 25°C[a] (kcal/mol)
Cyclohexane	8.2	80.7	7.93
Carbon tetrachloride	8.6	76.8	7.79
Toluene	8.9	110.6	9.08
Chloroform	9.3	61.2	7.20

[a] Calculated from Hindebrand equation [11]

calculated using the known cell parameters of orthorhombic polyethylene [11] ($a = 7.4$, $b = 4.93$, $c = 2.534$ Å with $\alpha = \beta = \gamma = 90°$) and using the relation [12]

$$d_{hkl} = [h^2/a^2 + k^2/b^2 + l^2/c^2]^{-1/2} \quad (4)$$

Indexing of reflections was done by comparing d_{hkl} values corresponding to different reflection peaks with the theoretically calculated d_{hkl} values. The interchain distance (R) was calculated using the relation [13]

$$R = \frac{5\lambda}{8 \sin \theta} \quad (5)$$

where λ is the wavelength of x-radiation [λ = 1.790 Å for Co-K_α].

2.6. Swelling measurements

The swelling measurement was made by immersing weighed test pieces of ~1 cm square and 0.2 mm thick, in redistilled 2,2,4 trimethyl pentane, which swelled the butadiene and hydrogenated butadiene portion only, but not the polystyrene portion [14]. The test pieces were carefully reweighed at approximately 24 h intervals until equilibrium swelling had been reached and maintained for 3–4 days. At least three test pieces were used from each film. The swelling index was calculated as follows:

$$\text{Swelling index} = \frac{\text{swollen mass}}{\text{original mass}}$$

2.7. Dynamic mechanical thermal analysis

The dynamic mechanical measurements were made using a Dynamic Mechanical Thermal Analyser (DMTA MK-II) from Polymer Laboratories, UK. All the samples (43.5 × 13.3 × 0.2 mm) were analysed in a dual cantilever bending mode with a strain of 64 μm (peak to peak displacement) in the temperature range from −120 to 50°C. The heating rate was 2°C/min and the frequency of the measurement was 10 Hz. DMTA MK II software (version 1.2) was used for data acquisition and analysis. The data were analysed using a COMPAQ Computer. The experimental error was ±1°C.

2.8. Measurement of physical properties

The tensile strength, elongation at break and modulus at 100% and 300% elongation were measured on dumb-bell specimens [(BS-E) type], cut with a hollow punch from the test sheet according to ASTM D-412-93 in a Zwick 1495 Universal Testing Machine at a strain rate of 500 mm/min at 25 ± 1°C. The averages of five data points were taken and the experimental error was ±5% (deviation from the median value).

3. Results and discussion

3.1. Viscosity study

Intrinsic viscosity [η], Huggins parameter, K_H and dimension of the polymer chains obtained from Eqs. (1)–(3) for HSBR in different solvents are reported in Table 3. These solvents were chosen as these are good solvents for polystyrene, butadiene and hydrogenated butadiene polymers. The highest intrinsic viscosity value indicates that cyclohexane is thermodynamically the most efficient solvent for HSBR. The increase in solubility parameter beyond cyclohexane makes the solvent thermodynamically less efficient and leads to smaller end-to-end distance of polymer chains. It is also found that there is no trend for K_H with change in solubility parameter of solvents, as reported earlier for SBR block copolymer [15]. The root mean square end-to-end distance is in line with the intrinsic viscosity data (Table 3).

3.2. SEM and TEM study

Transmission electron micrographs of various cast samples have been taken. A representative photograph of the sample cast from toluene is shown in Fig. 1a. Since the staining material (OsO_4) penetrates into the amorphous regions, the crystalline portions appear as white and the amorphous portions as black. Transmission electron micrographs of polyethylene, isotactic polypropylene and ethylene propylene copolymers have been reported earlier by Sano et al. [16]. The authors observed twisting lamellae of polyethylene and cross-hatched lamellae of polypropylene by staining the amorphous portions. The transmission electron micrographs of HSBR cast from toluene, CCl_4, cyclohexane and chloroform are similar at high magnification (10 000–30 000 ×). There is essentially no difference in the microstructure.

Scanning electron micrographs at lower magnifications, however, display distinct differences among various

Table 3
Viscosity and equilibrium swelling data of HSBR films

Film	Intrinsic viscosity (dl/g)	Huggin's constant	$(\bar{h}^2)^{1/2}$ (Å)	Swelling index
Cyclohexane cast	1.53	0.37 ± 0.03	252	4.6
Carbon tetrachloride cast	1.43	0.38 ± 0.03	246	5.1
Toluene cast	1.40	0.44 ± 0.02	244	5.9
Chloroform cast	1.26	0.31 ± 0.03	236	6.2
Compression moulded	—	—	—	6.5

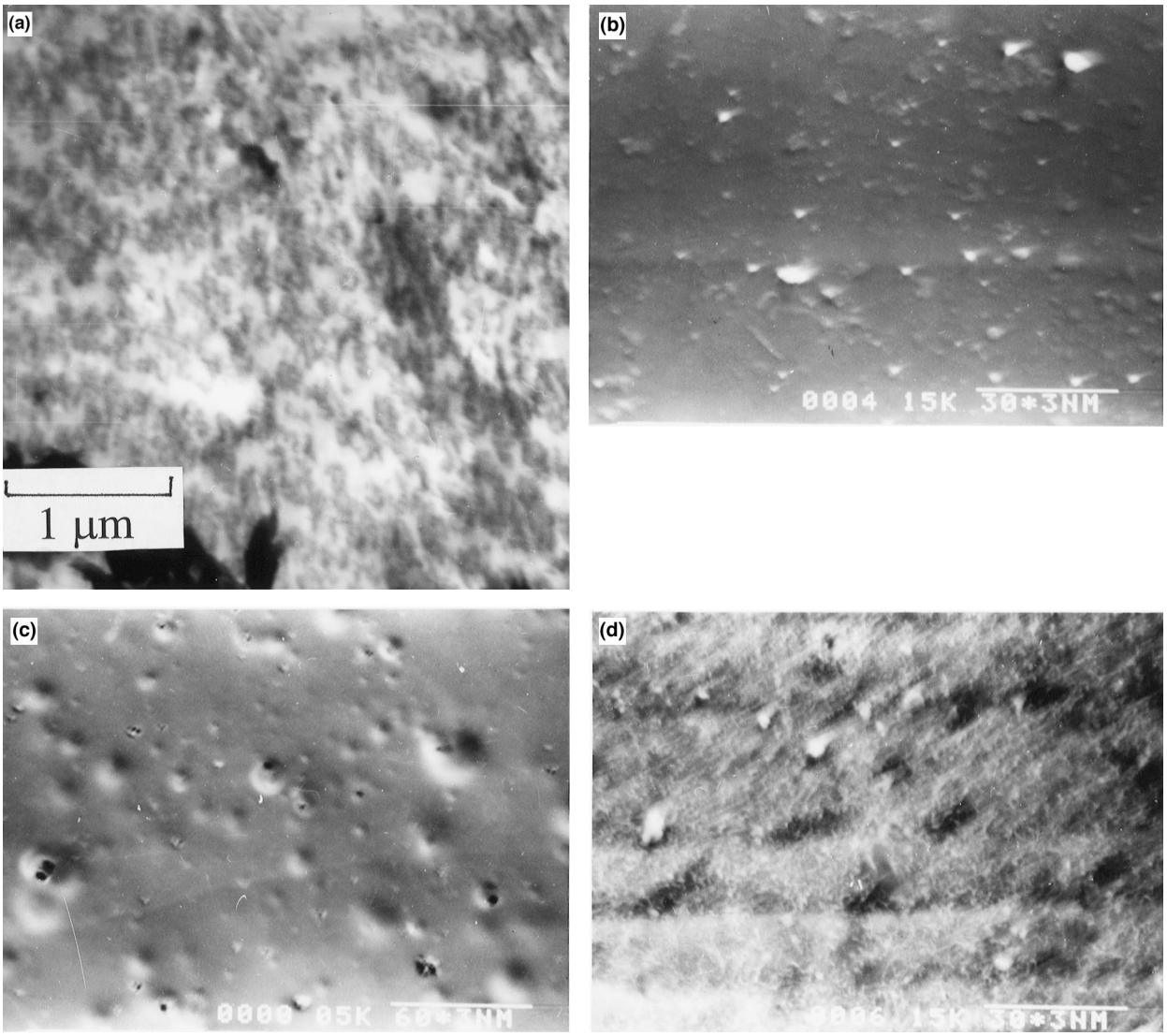

Fig. 1. (a) Transmission electron micrograph of HSBR film cast from toluene (25 000 ×); (b) Scanning electron micrograph of HSBR film cast from cyclohexane; (c) Scanning electron micrograph of HSBR film cast from chloroform; (d) Scanning electron micrograph of compression moulded film of HSBR.

samples. HSBR film cast from cyclohexane is featureless (Fig. 1b). There are a few white spots, which are not stained by OsO_4 (presumably the crystalline regions). There are also no voids. On the other hand, the chloroform cast sample shows a large number of microvoids and defects, possibly due to the fast evaporation rate of the solvent (Fig. 1c). The moulded samples, however, show different features (Fig. 1d) from the cast samples.

3.3. XRD results

X-ray diffractograms were recorded to characterise the

Table 4
X-ray diffraction studies

	Cyclohexane cast	Carbon tetrachloride cast	Toluene cast	Chloroform cast	Compression moulded film
2θ values	24.60	24.55	24.55	24.55	24.6
	27.65	27.55	27.50	27.15	—
Interplanar distance (A°)	4.20	4.21	4.21	4.21	4.20
	3.75	3.76	3.77	3.81	—
Interchain distance (A°)	5.25	5.26	5.26	5.26	5.25
	4.69	4.70	4.71	4.76	—
Degree of crystallinity(%)	7.6	6.4	6.2	4.8	7.9

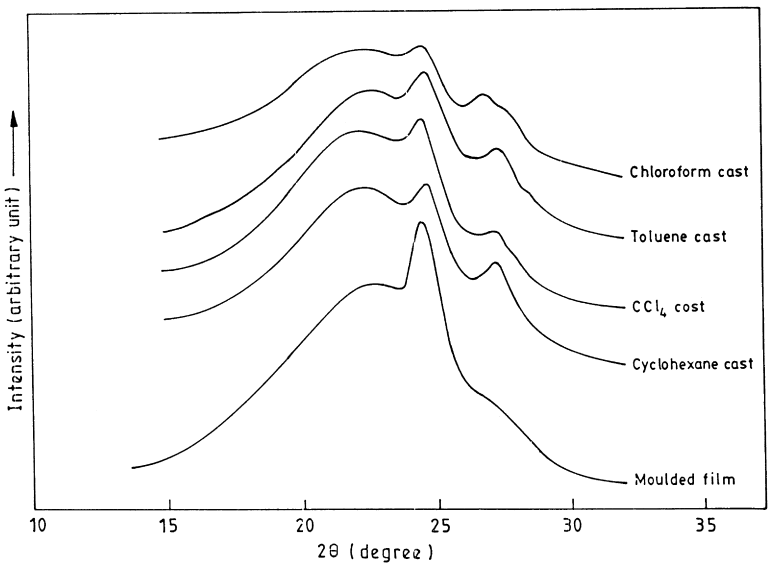

Fig. 2. X-ray diffraction patterns of HSBR films obtained under different conditions.

structure of HSBR films produced under different conditions. X-ray diffraction patterns for HSBR films prepared by solvent casting and compression moulding are shown in Fig. 2. A broad halo in the region from 15° to 30° 2θ represents the amorphous part. Compression moulded HSBR film shows a major reflection at 24.6° 2θ corresponding to (110) plane, which may be due to crystalline polyethylene segments. It is interesting to note that all solvent cast films display a new reflection at around 27.4–27.5° 2θ which may correspond to (200) plane. It is reported that low density polyethylene displays major reflections from both (110) and (200) planes [17]. The parameters evaluated from the x-ray diffractograms are reported in Table 4. It is seen that the increase in interplanar/interchain distance along (200) plane also indicates loose packing of polymer chains beyond cyclohexane. An abrupt decrease in crystallinity is also observed in this series. The much lower crystallinity value (4.8%) of chloroform cast films may be due to poorer quality of chloroform as a solvent for HSBR and also due to the higher rate of evaporation (heat of evaporation being the lowest for chloroform, Table 2) which inhibits the formation of crystallites leading to a porous films with a low crystallinity value.

3.4. Swelling experiments

As it is known that 2,2,4 trimethyl pentane swells butadiene and hydrogenated butadiene, but not the polystyrene portion, it may then be used to ascertain whether casting solvents have any significant effect on equilibrium swelling. The data in Table 3 clearly show that the chloroform cast film and compression moulded film absorb distinctly more swelling liquid, whereas the cyclohexane cast film swells least. As cyclohexane is thermodynamically the best solvent (see [η] in Table 3) for HSBR, the polymer, therefore, exists in a relatively extended chain configuration in cyclohexane. We assume that the polymer will deposit in a similar configuration on to the glass substrate [18] and will tend to form into tightly packed void-free films. This is also reflected in the x-ray structure. As a result, the solvent penetration is somewhat restricted, giving rise to a low swelling index. In thermodynamically less efficient solvents, such as chloroform, the chains are more tightly coiled, intramolecular interactions will be favoured over intermolecular linkages and a more porous film structure may be postulated [19]. SEM photographs shown in Fig. 1b and Fig. 1c illustrate these points. The chloroform cast film displays microvoids on the surface.

3.5. Dynamic mechanical thermal analysis

Dynamic mechanical properties of solvent cast films are displayed in Fig. 3a and Fig. 3b. All the HSBR films display a strong transition at −22 to −23°C. This peak is ascribed to the glass transition temperature (T_g) of HSBR which remains the same (the position of peak is recorded as being accurate to ±1°C) and independent of the nature of the solvent. A weak transition at around −108°C is seen in all cases which may be due to crank shaft motion in the molecular chains of $-CH_2$ units of HSBR. Table 5 shows the glass transition temperature and the influence of solvent on the peak tan δ and storage modulus (E') at T_g. Peak tan δ

Table 5
Dynamic mechanical properties of HSBR films

Film	T_g (°C)	Peak tan δ	$E' \times 10^{-11}$ (Pa)at T_g
Cyclohexane cast	−23	0.36	0.50
Carbon tetrachloride cast	−22	0.42	0.22
Toluene cast	−23	0.43	0.21
Chloroform cast	−23	0.34	0.14
Compression moulded	−22	0.42	0.26

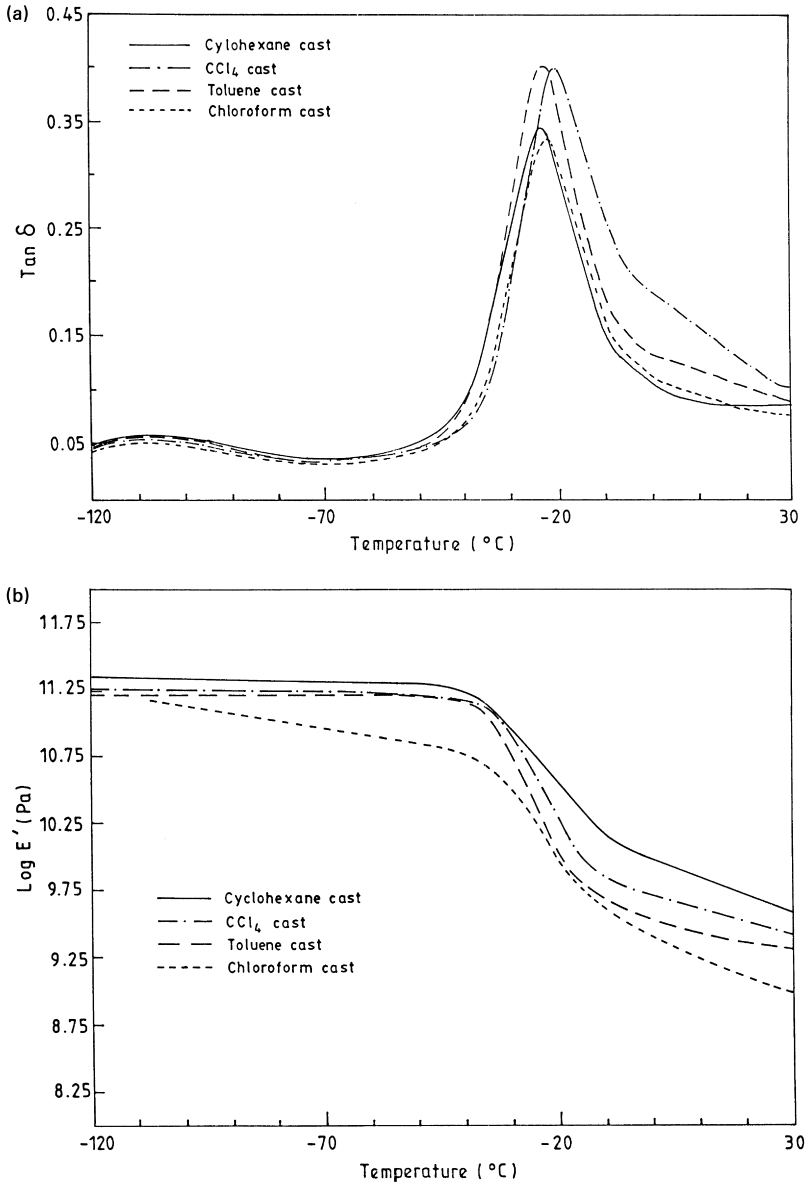

Fig. 3. (a) Temperature dependence of loss tangent (tan δ) for HSBR film cast from cyclohexane, CCl_4, toluene and chloroform, at a frequency of 10 Hz; (b) Temperature dependence of storage modulus (E') for HSBR film cast from cyclohexane, CCl_4, toluene and chloroform at a frequency of 10 Hz.

decreases from 0.43 for toluene to 0.36 for cyclohexane, because of its higher crystallinity and closer packing, as observed from x-ray study and void-free film shown in SEM photographs. However, the compression moulded samples register a lower modulus value and a higher tan δ_{max} (not shown in the figure, as the curve closely superimposes on that of the toluene cast film). This may be due to the occurrence of voids during compression moulding technique shown in Fig. 1d. An anomalous behaviour for chloroform cast film is observed. The tan δ_{max} of chloroform cast film is found to be lowest in spite of its lowest crystallinity and porous film structure. This may due to the fastest evaporation rate of chloroform. The influence of evaporation rates is discussed in a later section. The peak tan δ at -108°C, however, does not change significantly with the nature of the solvent.

It is also observed that the cyclohexane cast films show the highest storage modulus at the glass transition temperature. The tan δ of cyclohexane cast films, which is the ratio of E''/E' is lower because of higher values of E'. In the plot of log E' versus temperature (Fig. 3b), the cyclohexane cast film displays the highest modulus over the whole range of temperatures. The modulus values of films cast from other solvents are in line with the crystallinity reported in Table 4.

3.6. Mechanical properties

Fig. 4 shows the stress–strain behaviour of different

Table 6
Mechanical properties of solvent cast films

Films	Cyclohexane cast	Carbon tetra chloride cast	Toluene cast	Chloroform cast	Molded film
Tensile strength (MPa)	10.2	7.2	6.7	6.2	9.4
Elongation at break (%)	1050	1010	1013	982	1000
Work to break (kJ/m^2)	22.3	15.1	14.5	13.9	19.4
Modulus (MPa)					
100%	1.51	1.46	1.35	1.30	1.50
300%	2.56	2.42	2.20	2.18	2.68
Total energy function[a]	10.7	7.3	6.8	6.1	9.4

[a] Total energy function ⇒ Tensile strength × elongation at break × 10^{-3}

solvent cast HSBR films. All the films show typical rubbery characteristics with a low modulus and high elongation value. But, it can be seen that the mechanical behaviour is very much dependent upon the manner in which the samples have been prepared. The effect of casting solvents on the physical properties of the films is displayed in Table 6. It is observed that cyclohexane cast films show superior mechanical properties compared to the other solvent cast systems. The superior mechanical properties can be explained satisfactorily in terms of its relatively high crystallinity. Another reason is that, in cyclohexane, a tightly packed film with smaller interplanar and interchain distances is formed, as evidenced from its high swelling resistance. Also, there is no void. So, high energy is required for failure, resulting in a higher ultimate tensile strength. The tensile behaviour is again related to work done, which may be calculated from the area under the stress–strain curve as in Fig. 4. For a linear material, the strain energy or work is given by half of the product of stress and strain. Hence, at a constant strain, the higher the work, the higher will be tensile stress. The modulus values for 100 and 300% elongation are also higher for cyclohexane cast films due to the same reason as described above. It is interesting to note that the film cast from cyclohexane displays even higher mechanical properties than the moulded films. Chloroform cast films show poor mechanical properties because of its porous nature and low crystallinity. The tensile stress is inversely proportional to the flaw size.

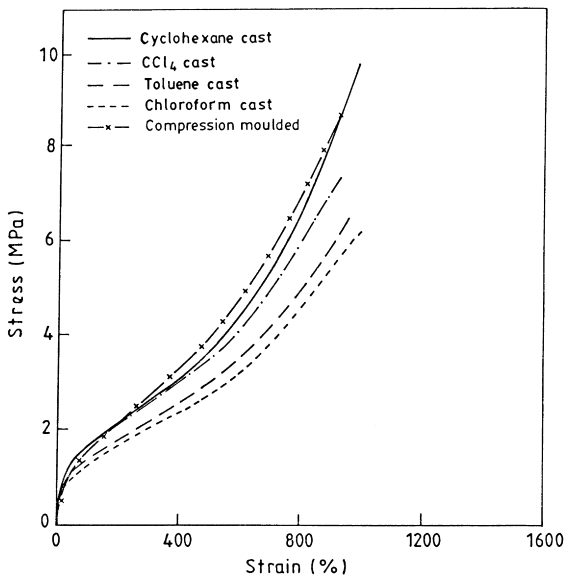

Fig. 4. Stress–strain curves for HSBR films obtained under different conditions.

3.7. Influence of rate of solvent evaporation on film properties

A limited investigation of the influence of solvent evaporation rate on the resulting physical properties of the cast film was undertaken. Carbon tetrachloride was chosen as the casting solvent because of its moderate rate of evaporation. A change in the solvent evaporation rate from 5 to 50 ml/h causes a change in the crystallinity. The values of degree of crystallinity of cast films as evaporated at 5, 25 and 50 ml/h are 6.4, 5.7 and 5.1, respectively. The tensile strength, elongation at break, work to break and modulus values also decrease with increase in rate of evaporation (Table 7). Fig. 5 shows an interesting point that the width and peak height of the tan δ are sensitive to solvent evaporation rate. The glass transition almost remains unchanged, whereas the tan δ value decreases with increase in evaporation rate. The tan δ_{max} values of the films are 0.43, 0.38 and 0.33 when the evaporation rates are 5, 25 and 50 ml/h, respectively. A similar observation was made earlier, although the peak positions were reported to be shifted to higher temperatures with increase in evaporation rate [14].

Table 7
Effect of rate of solvent (CCl_4) evaporation on physical properties of cast films

	Rate of solvent evaporation		
	5 ml/h	25 ml/h	50 ml/h
Crystallinity (%)	6.4	5.7	5.1
Tensile strength (MPa)	7.2	6.8	6.4
Elongation at break (%)	1010	981	956
Work to break (kJ/m^2)	15.1	14.9	13.8
Modulus (MPa)			
100%	1.46	1.36	1.31
300%	2.42	2.25	2.10

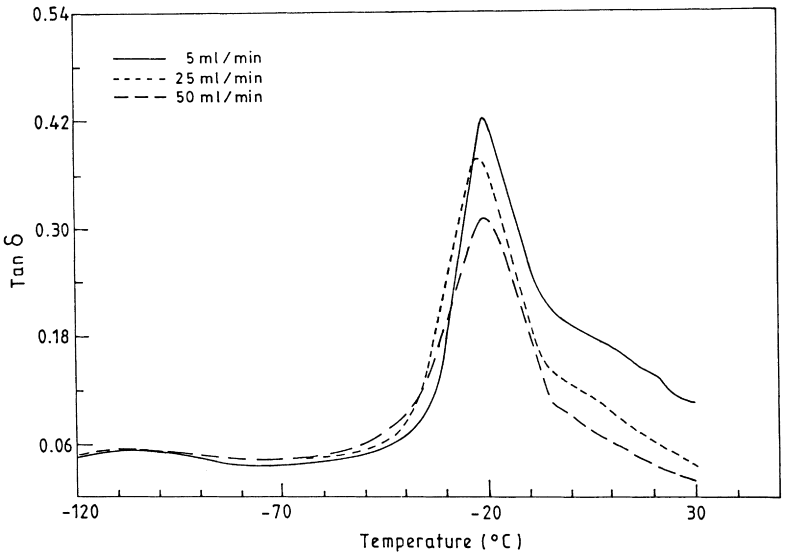

Fig. 5. Temperature dependence of loss tangent (tan δ) for HSBR cast from carbon tetrachloride at 5, 25 and 50 ml/h at a frequency of 10 Hz.

4. Conclusions

The influence of casting solvents on the properties of hydrogenated styrene–butadiene copolymer has been investigated in this paper:

1. The highest intrinsic viscosity value is indicative of the fact that cyclohexane is thermodynamically the most efficient solvent for HSBR. The increase in solubility parameters beyond cyclohexane reduces the intrinsic viscosity.
2. The structure of the films as observed by SEM is different for different samples. The chloroform cast sample shows microvoids and defects.
3. X-ray studies also indicate the closest packing in cyclohexane cast films [interplanar/interchain distance along (200) plane being the lowest]. The degree of crystallinity decreases with increase in solubility parameters beyond cyclohexane.
4. Dynamic mechanical thermal analysis shows that the temperature at which tan δ reaches maximum is essentially constant, whereas, the peak tan δ height is influenced by the nature of the solvents. Higher storage modulus values are observed for cyclohexane over the whole range of temperatures.
5. The cyclohexane cast films are found to be superior to other solvent cast films in terms of mechanical properties. The results are explained on the basis of its high crystallinity and close packing.
6. The properties of solvent cast films are dependent on the rate of evaporation of casting solvents. The crystallinity and the mechanical properties decrease with increase in evaporation rate. The peak tan δ value also decreases with increase in evaporation rate.

Acknowledgements

One of the authors (Mousumi De Sarkar) is grateful to CSIR, New Delhi for providing a research fellowship to carry out the work.

References

[1] Bhowmick AK, Stephens HL. In: Handbook of elastomers. New York: Marcel Dekker, 1988.
[2] Parker DK, Roberts RF, Schiessel HW. Rubber Chem Technol 1992;65:245.
[3] Parker DK, Roberts RF, Schiessel HW. Rubber Chem Technol 1994;67:288.
[4] De Sarkar M, De PP, Bhowmick AK. J Appl Polym Sci 1997;66:1151.
[5] De Sarkar M, Mukunda PG, De PP, Bhowmick AK. Rubber Chem Technol, 1997;70:855.
[6] Flory PJ. In: Principles of polymer chemistry. Ithaca, NY: Cornell University Press, 1953.
[7] Huggins ML. J Appl Chem Soc 1942;64:2716.
[8] Kraemer EO. Ind Eng Chem 1938;30:1200.
[9] Smith DR, Meier DJ. Polymer 1992;33:3779.
[10] Suehiro S, Yamada T, Inagaki H, Kawai H. Polym J 1978;10:315.
[11] Miller RL. In: Bandrup J, Immergut EH, editors. Polymer handbook. New York: Wiley Interscience, 1989.
[12] Stallon WO. In: Kaelble EF, editor. Handbook of x-ray diffraction, emission, adsorption and microscopy. New York: McGraw-Hill, 1967, Ch. 21.
[13] Klug A, Alexander LF. X-ray diffraction procedures. New York: Wiley, 1969.
[14] Beamish A, Goldberg RA, Hourston DJ. Polymer 1977;18:49.
[15] Enyiegbulam M, Hourston DJ. Polymer 1979;20:818.
[16] Sano H, Usami T, Nakagawa H. Polymer 1986;27:1497.
[17] Kole S, Santra R, Chaki TK, Samantray BK, Tripathy DK, Nando GB, Bhowmick AK. Polym. Networks Blends 1995;5 (3):117.
[18] Funke W. J Oil Col Chem Assoc 1976;59:398.
[19] Boberski WG. Ind Eng Chem Prod Res Dev 1975;14:139.